THE INCAS PROJECT: AN INNOVATIVE CONTACT-LESS ANGULAR SENSOR

L. Ghislanzoni [(1)], A. Di Cintio [(2)], M. Solimando [(2)], G. Parzianello[(3)]

[(1)] C-Sigma srl, Via Cavour 18, 23900 Lecco (Italy), Email: luca.ghislanzoni@c-sigma.it
[(2)] CGS SpA, Via Gallarate 150, 20151 Milano (Italy), Email: adicintio@cgspace.it, msolimando@cgspace.it
[(3)] ESA/ESTEC, Keplerlaan 1, 2201 AZ Noordwijk (The Netherlands), Email: giorgio.parzianello@esa.int

ABSTRACT

Angular Positions sensors are widely used in all spacecrafts, including re-entry vehicles and launchers, where mechanisms and pointing-scanning devices are required. The main applications are on mechanisms for TeleMeasure (TM) related to the release and deployment of devices, or on rotary mechanisms such as Solar Array Drive Mechanism (SADM) and Antenna Pointing Mechanism (APM). Longer lifetime (up to 7-10 years) is becoming a new driver for the coming missions and contact technology sensors often incur in limitations due to the wear of the contacting parts [1].
A Self-Compensating Absolute Angular Encoder was developed and tested in the frame of an ESA's ARTES 5.2 project, named INCAS (INnovative Contact-less Angular Sensor). More in particular, the INCAS sensor addresses a market need for contactless angular sensors aimed at replacing the more conventional rotary potentiometers, while featuring the same level of accuracy performances and extending the expected lifetime.

1. INTRODUCTION

The most widely adopted solutions to measure the angular position in a variety of mechanisms on board spacecrafts are based on optical encoders.
However making this type of devices rugged against the severe vibrations environment experienced during launch, against the radiation environment during the flight mission, and extending their operational temperature range, has so far often resulted in very expensive products.
Angular sensors based instead on the use of sliding contact rotary potentiometers, provide an interesting lower cost alternative when the required accuracy is less demanding, but are sometimes not matching the level of reliability and/or durability required.
In addition, due to current space industry trend to substitute potentiometers with longer lasting type of sensors [2] [3] [4] in applications where a long service life is needed, a product based on a contactless technology (such as the one implemented in INCAS) will likely be of interest for several coming applications where the lifetime is the key driving requirement.
With a conservative approach, it is assumed that initially INCAS could be used for applications requiring average performance sensors.
There actually exist needs for an angular sensor, which shall be:

- mechanically robust;
- rugged against radiations;
- insensitive to wide temperature variations under space vacuum conditions;
- inherently low cost;
- long life performance

The main starting point of the INCAS project is the output of the ITI-CAS project, carried out by Carlo Gavazzi Space (now CGS S.p.A., an OHB Company) and C-Sigma, under an ESA Contract.

The basic concept had originally been developed by C-Sigma, for rugged industrial and transportation applications (patent pending).

2. MAIN FEATURES

The product developed is an Absolute Angular Encoder, including Signal Conditioning Electronics, suitable for the space environment, and characterized by the following features:

- Self-compensating configuration of Hall effect probes.
- Rotary Magnetic Design inherently storing angle position (no stand-by current needed to retain position information).
- Purely analogue signal processing (no software);
- Cost effective.
- Accuracy = ± 0.5°.
- Repeatability = ± 0.1°.
- High resolution.

The INCAS absolute encoder aims at satisfying these requirements by means of a contact-less sensor. This is the main characteristic that differentiates the INCAS approach with respect to the currently used sliding contact type of sensors, yielding thus a more robust and reliable solution, especially over long life missions.
The low cost approach of this sensor is intended to provide also a convenient alternative to more expensive sensors for this class of performance.

The dedicated electronics shall be fully redundant and all the parts for the Engineering Model prototype, as well as for the Qualification Model foreseen in the next phase, are ITAR free.

3. GENERAL DESCRIPTION

The INCAS sensor is composed of a Stator part and a Rotor part. The Stator will be mated to the flange of the rotary mechanism, while the Rotor will be coupled to the shaft of said rotary mechanism. Fig. 1 and Fig. 2 illustrate how Rotor and Stator are two completely separable parts.

Figure 1. The Rotor separated from the Stator

Figure 2. The Rotor inserted into the Stator.

The total number of probes is 8, i.e. 4 pairs of diametrically opposed matched probes, and each probe is glued in a milled cavity (see red circle in Fig.2). In this way we obtain one set of two orthogonal Main pairs plus one set of two orthogonal Redundant pairs. Also the PCBs are split into two identical halves. Hence, the final product is a fully redundant Absolute Angular Position Sensor.

4. PRINCIPLE OF OPERATION

The principle of operation exploits a biasing permanent magnet generating a magnetic field in an air-gap of suitable geometry, and whose value is a function of the angular position. Hall effect probes are located at diametrically opposed positions along the air-gap.

The magnetic circuit configuration is such that the angular position is a function of the ratio between the magnetic field value measured by one individual Hall probe, $B(\vartheta)$, and its arithmetic mean with the value, $B(\vartheta+\pi)$, measured by the diametrically opposed matched probe.

In this way any drift or degradation of the permanent magnet or Hall probes characteristics is automatically self-compensated by the usage of the ratio of the sensed magnetic field (both probes) and thanks to a closed loop feedback for the probes supply (see Fig.4). Indeed, the angular position is a function of geometric relationships only, making the sensor insensitive to degradation effects and drifts of parameters. Fig. 3 illustrates the rotary magnetic circuit at the base of the principle of operation.

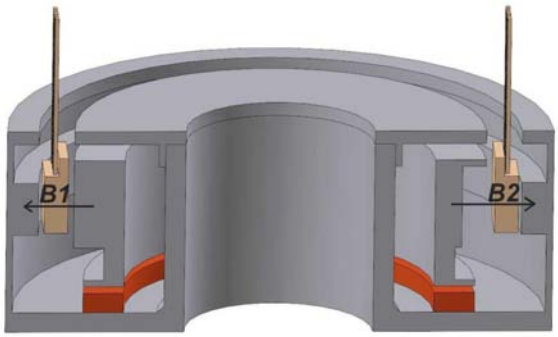

Figure 3 – The variable rotary airgap.

Two matched Hall effect probes (orange) are located at diametrically opposed angular positions, inside the main airgap of the rotary magnetic circuit (grey), and in which a static magnetic field is established thanks to the presence of a permanent magnet (red). The radial width of the airgap is a function of angular position, designed to obtain a constant mean value of the measurements of the two probes, independently from the angular position:

$$B_{virtual} = \frac{B(\vartheta) + B(\vartheta + \pi)}{2} \qquad (1)$$

This effectively acts as a *Virtual Reference Airgap* of constant width, whose magnetic field value conveys information about drifts with temperature of the permanent magnet characteristics, as well as about all those geometrical variations affecting the overall reluctance of the magnetic circuit.

For *matched* Hall probes of the ratiometric type (i.e. whose magnetic sensitivity is proportional to the bias current or supply voltage), it is then possible to implement a feedback loop (see Fig. 4) actively adjusting the supply to the probes (thus, their magnetic sensitivity), as to guarantee that:

$$\frac{V_{h1} + V_{h2}}{2} = V_{ref} \qquad (2)$$

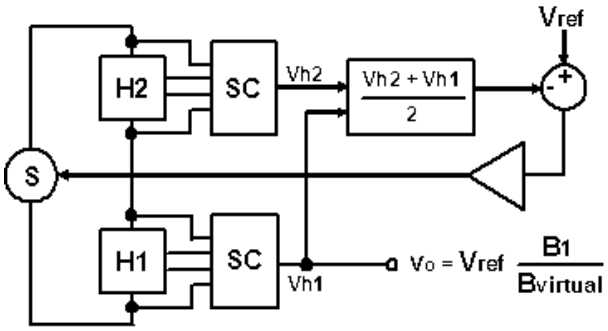

Figure 4. The feedback loop computing B1/(B1+B2).

In this way the feedback loop automatically generates the value of the ratio representing the self-compensated function of angular position we were aiming for:

$$f(\vartheta) = v_O = V_{ref}\frac{B(\vartheta)}{B(\vartheta)+B(\vartheta+\pi)} \qquad (3)$$

The v_o output now depends on geometric relationships only (variation of $B(\vartheta)$ along the revolution), having become substantially independent from any drift with temperature of the working point of the permanent magnet, as well as from common mode drifts in the sensitivity of the Hall probes.

5. MAGNETIC DESIGN

The radial profile of the inner yoke of the circular airgap has been carefully designed with the aid of FEA magnetostatics simulations. Fig. 5 illustrates an example of the output generated by such simulations (Magnum 3.1 from Field Precision: with uniform mesh of 0.1 mm element size, for a total of about 30 million elements). The profile of the magnetic circuit has been optimised to maximise the uniformity of the magnetic field in the airgap both radially and axially, in order to reduce the sensitivity to potential misalignments during the probes mounting.

The magnetic profile yields the two $f(\vartheta)$ functions represented in Fig. 6 (green and blue), and which coincide with the signal V_{h1} and V_{h2} of the pair of probes bound together by the feedback loop of Fig. 4.

The solid black line represents their arithmetic mean, exactly equal to the 5V reference voltage (an Analog Device's REF02 precision voltage reference).

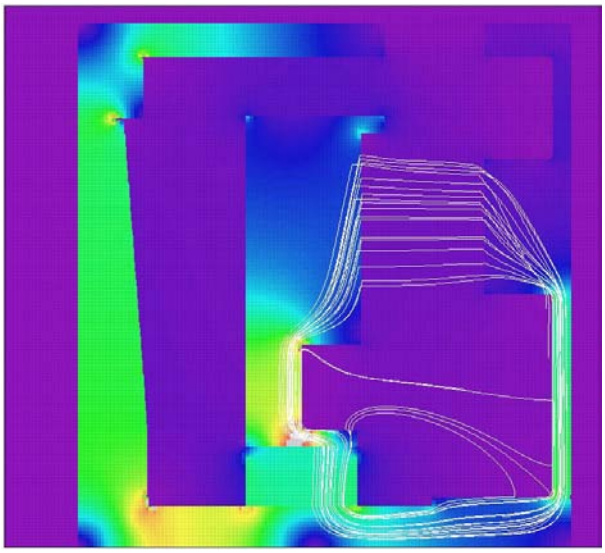

Figure 5. Example of FEA simulations output

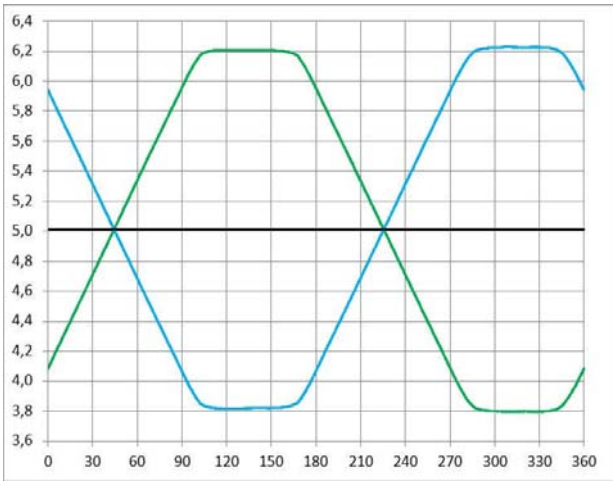

Figure 6. The V_{h1} (green) and V_{h2} (blue) signals of Fig. 4, for probes belonging to the same pair (vertical scale in Volts).

It is clear that the two signals in Fig. 6, not being independent from each other, are by themselves not sufficient to univocally identify the rotor's angular position over the full 360° revolution. This is the reason why a second pair of probes needs to be added at 90° angular distance, in order to generate the necessary quadrature signal. The red trapezoid in Fig. 7 represents the V_{h1} signal from the second pair of probes (also bound together by their own feedback loop, identical to the one used for the first pair).

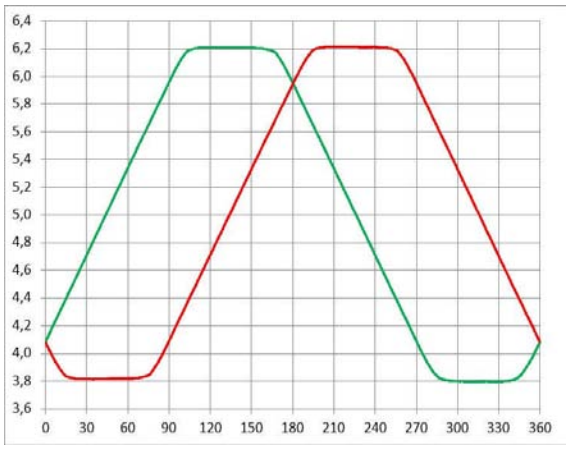

Figure 7. V_{h1} of Fig. 6 together with the V_{h1} signal (red) from the pair of probes at 90° (vertical scale in Volts).

6. PROBES MATCHING

In order to take full advantage of the self-compensating features of the principle of operation, it is crucial to match the drifts of the magnetic sensitivities of paired probes. This is usually the case for probes belonging to the same wafer lot. However, it is possible to further improve the performance of the sensor by characterizing in temperature each individual probe, and then pairing the ones with the most similar temperature drift coefficients.

Fig. 8 illustrates typical drifts with temperature (relatively to the value at 25°C) of the magnetic sensitivities of matched pairs. Although the absolute value of their respective magnetic field sensitivity drifts by about +/- 3% (red and green curves), the relative variation of the matched probes remains within 0.1% (blue curve). The measurements refer to OPTEK OMH3150 Linear Hall Effect Probes.

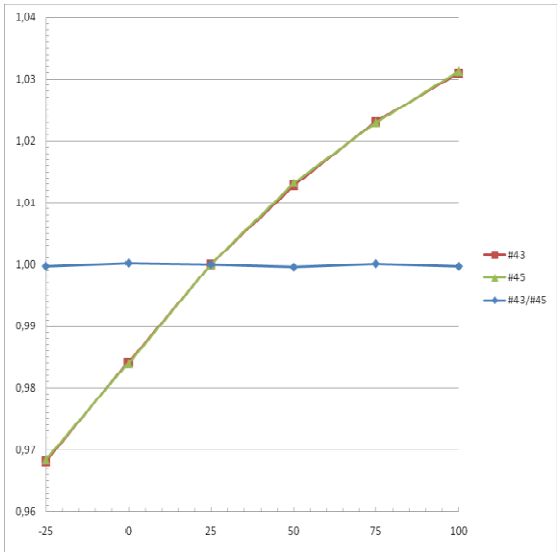

Figure 8. Example of probes sensitivities matching.

Furthermore, each probe is characterized also by a zero field offset (i.e. its output signal when B = 0), that also drifts with temperature, requiring therefore compensation. A specific circuitry has thus been added to compensate the linear part of the zero field offset drift with temperature.

A probes selection procedure has been implemented, focussing both on the linearity of the respective zero field offset drifts with temperature and on the matching of the sensitivity drift among pairs of probes.

The compensation circuitry for the temperature linear dependence of the zero field offset benefits from the reading of the temperature transducer built in the precision reference voltage IC utilized (REF02 from Analog Device). The REF02's TEMP output, is also buffered and routed to one of the output pins of the connector of INCAS.

Thanks to the fact that the Hall probes sit in the middle of the rotary airgap, and are thus surrounded by several mm of 430F stainless steel and/or Al, we have estimated that in a typical Geostationary Earth Orbit Environment this shielding effect will result in about a factor 10 reduction of the Total Ionizing Dose (TID) with respect to the TID dose received by components located outside. This design, together with the automatic rejection of common drifts (including the ones due to TID) for the two probes, improves significantly the radiation resistance of the sensor

Furthermore, we have just started to characterize some recent GaAs linear Hall probes from ASAHI KASEI Microdevices (HG-362A). The preliminary results about intra-lot matching, and extent of the zero field offset temperature drift, are very encouraging. Being based on a simple GaAs die, without any other signal conditioning and processing circuitry on the die, these probes are, in principle, expected to feature a high TID tolerance.

7. OUTPUT SIGNAL OPTIONS

Each of the four linear segments of the native trapezoidal signals of Fig. 7 can be recombined and used to identify, without ambiguity, the actual angular position along the entire revolution. This would give an output 0-5 V covering the entire 360 degrees.
Because the most linear portions of the two trapezoids in Fig. 7 are the four sides, an optimal signal processing algorithm, implemented at the OBDH (On Board Data Handling) System side, would select for the four 90° arcs corresponding to the central segments (from about 4V to about 6V) of said four trapezoids sides.
Alternatively, for some high accuracy applications requiring a best signal/noise ratio, the output signal waveforms of Fig. 9 might actually represent a better compromise.

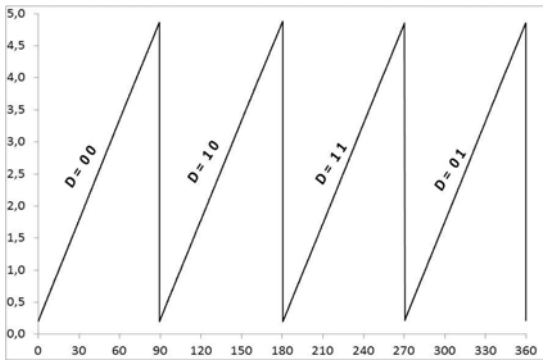

Figure 9. Our choice of optimal output signal waveform.

Each one of the sawtooth's four ramps covers a 90° arc of angular positions. Each ramp is selected directly from the signals already available at the 4 outputs (V_{h1} and V_{h2} of one pair, and V_{h1} and V_{h2} of the orthogonal pair) of the two feedback loops. The selection is accomplished by means of two comparators and one analog multiplexer. The comparators' outputs are used for switching the analog multiplexer from one trapezoid's side to the next, but they are also routed as digital signals to two outputs of the sensor (the digital coding identifies the angular sector in use). The advantages of such an approach are:

- A user would need to allocate to the angular position sensor only one analog input channel (usually more at premium than digital ones), instead of two as it would be the case for Fig.7.
- The two digital channels then Gray code for the particular 90° arc (0° to 90°, 90° to 180°, 180° to 270°, or 270° to 360°), as for code D in Fig. 9.
- In this way, the full 0-5V input range of an analog input channel can be exploited to cover just 90°, instead of the full 360°, effectively quadrupling the resolution of the A to D conversion (with respect to the more conventional approach of just one 0-5V ramp covering the full 360°).

Furthermore, the signal processing algorithm computing the angular position in degrees, starting from the output voltage in Volts, will in such case assume a very simple form: just a set of 4 equations (*i = 1, 2, 3, 4)*

$$\vartheta = A_i \ (V_{out} - B_i) \qquad (4)$$

Whereby the B_i represent the zero field offset for each segment of the output signal, and the A_i the respective slopes. The algorithm will then switch from one equation to the next based on the value of the digital Gray code D. For the most accurate applications it could then be possible to use the 8 functions describing the temperature dependence of each one of the A_i and B_i coefficients. Alternatively, it is also possible to electronically combine, inside INCAS, the four ramps of Fig. 9 into a single 0V – 5V linear ramp, covering the full 0°-360° revolution.

8. PERFORMANCES

In order to assess the detailed performances of our newly developed sensor, we submitted it to a full set of measurements and verifications, among which:

- Absolute Accuracy, and its temperature dependence
- Repeatability
- Sensibility to Rotor-Stator relative misalignments
- Vibration Testing
- Thermal Vacuum Cycling
- EMC and EMI Testing

Within the space available for this publication it is impossible to thoroughly review all the results of the Test Campaign. We will therefore limit our summary to the most relevant performance parameters.
Several different Rotors where measured, and with different Stators. Fig. 10 illustrates just an example for the absolute error typically observed (deviation in degrees from the actual position as measured by an accurate reference encoder, over the full 0-360° revolution). The detailed shape of the green curve varies from rotor to rotor, and it is related to the intrinsic machining accuracy of the profiled cam corresponding to the inner yoke of the rotary airgap of Fig. 3. Most would be contained within ± 0.3° maximum deviation (as for the example in Fig. 10), but few would even achieve an excellent ± 0.15° maximum deviation.

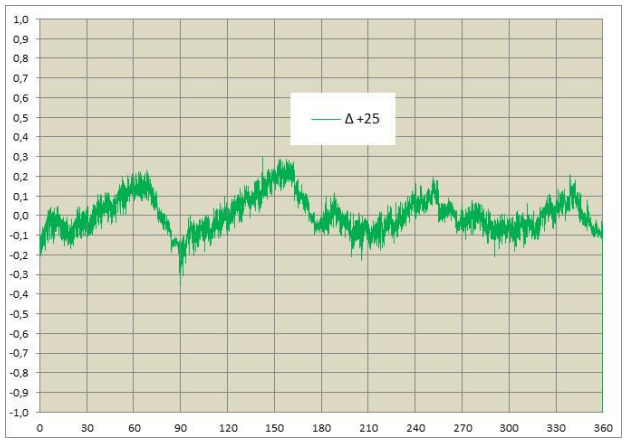

Figure 10. Total absolute error (in degrees) over the full 0-360° revolution, at 25°C.

Fig. 11 then illustrates how the absolute error drifts with temperature. Such drift represents the residual amount left after the internal compensation of the zero field offset drift with temperature, and it is slightly different for each one of the four segments of Fig.9 (i.e. the four Hall probes). It results in a total error anyway contained within ± 0.5°, over the full -30°C to +100°C range.

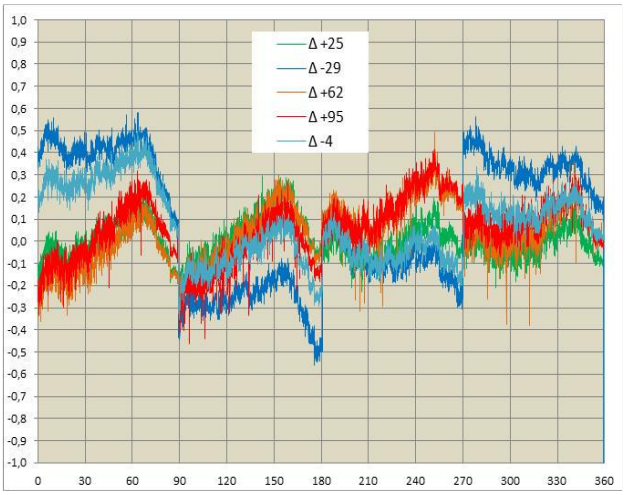

Figure 11. Absolute error over the full temperature range.

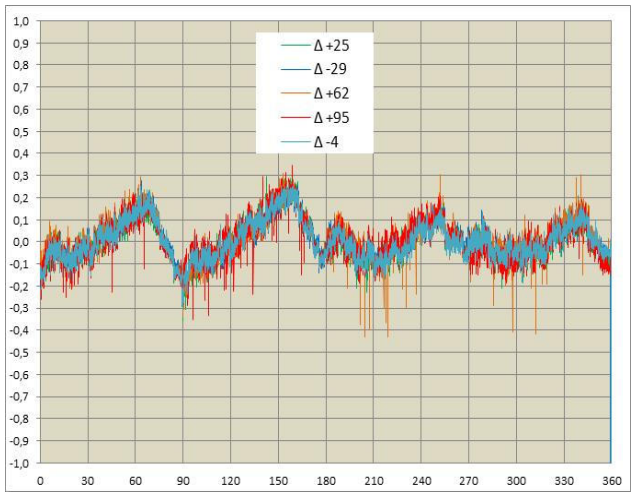

Figure 12. *Fine T drift Post Compensation* applied to Fig. 11 Data

In Fig. 11, the conversion equations applied for each one of the four segments of the output signal depicted in Fig. 9 are:

$$D = 00 \quad \rightarrow \quad \vartheta = 19.19\ (V_{out} - 0.217)$$

$$D = 10 \quad \rightarrow \quad \vartheta = 19.47\ (V_{out} - 0.242) + 90°$$

$$D = 11 \quad \rightarrow \quad \vartheta = 19.30\ (V_{out} - 0.175) + 180°$$

$$D = 01 \quad \rightarrow \quad \vartheta = 19.24\ (V_{out} - 0.196) + 270°$$

and whereby all the eight coefficients are held constant with temperature.

As already explained above, for applications requiring the outermost accuracy, the differing drifts with temperature of each one of the four segments could then further be "*fine compensated*" by using a table of values describing the temperature dependence of each one of the A_i and B_i coefficients. For such a "*Fine T Drift Post Compensation*" a look-up table can be provided. Interpolation could then be considered for intermediate temperature values. Fig. 12 illustrates the excellent temperature drift compensation achievable by applying said "*Fine T Drift Post Compensation*" to the data of Fig. 11. The reference temperature value is the value measured, internally to INCAS, by the REF02 temperature transducer, and made available at one of the output pins of the connector of our Absolute Angular Position Sensor.

Finally, Fig. 13 demonstrates an excellent repeatability (superposition of full revolutions recorded after several other intervening full revolutions) within ± 0.0015°.

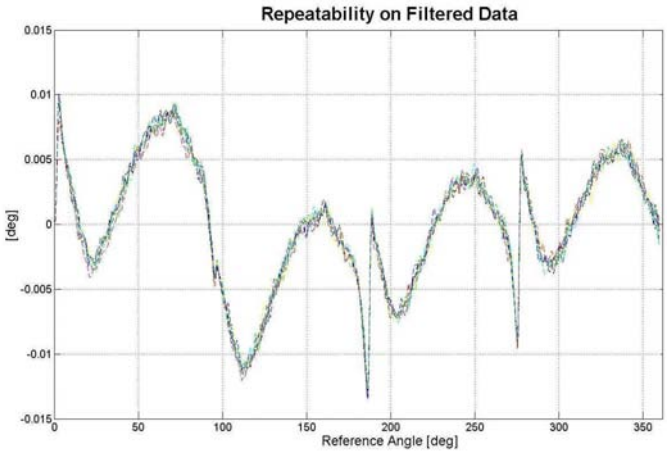

Figure 13. Repeatability

9. CONCLUSIONS

The INCAS Self-Compensating Hall Effect Absolute Angular Sensor is capable of achieving, and in some cases exceeding, the performances of conventional rotary potentiometers.

For applications requiring the outermost accuracy, the verified "*Fine T Drift Post Compensation*" can be applied in order to decrease the typical -30°C to 100°C temperature drift down to negligible values, so that the overall accuracy becomes largely dominated by the intrinsic linearity error (due to the cam profile machining inaccuracies).

On the other end, we have also verified that said intrinsic linearity error is very stable and that it features

an excellent repeatability. Thus, once fully characterized, it could also be compensated for by implementing a suitable post-processing algorithm.

The following list summarizes the most important key characteristics we were able to verify:

- Absolute Error @ 25°C ±0.3°
- Absolute Error -30 to 100°C ±0.5°
- Repeatability Error: ± 0.02°
- Resolution: analog output
- Output Signal: various options
- Supply: 12V to 15V, 40mA
- Stator mass: 65 gr
- Rotor mass: 60 gr
- Internal Temperature available at a connector pin
- Hollow shaft configuration with 14 mm diam. bore
- Fully Redundant
- 100krad TID radiation tolerance for GEO orbits
- Operating temperature range: -55°C to +125°C

10. REFERENCES

1. Wood, B., Musset, D., Cattaldo, O. & Rohr, T. (2005). SADM Potentiometer Anomaly Investigations. *Proc. Of the 11th ESMATS, 2005.* ESA SP-535, European Space Agency, Noordwijk, The Netherlands.

2. Sache, L. Reymond, C., Keijk, P., Sjöholm, M., Bommottet, D., Gass, V., Gaillard, L. & Popovic, R.S. (2008). Circular Hall Transducer for Accurate Contactless Angular Position Sensing. *Proc. Of the 39th Aerospace Mechanisms Symposium, 2008.* NASA-CP-2008-2152520.

3. Kottmeier, S., Müller, S., Schmidt, T., Zajac, K. & Schmallbach, M. (2011). A High-Precision, High-Reliability Binary Rotary Encoder Using Hall-Effect Sensors. *Proc. Of the 14th ESMATS, 2011.* ESA SP-698, European Space Agency, Noordwijk, The Netherlands.

4. Talvat, T., Grass, A., Gibard, D., Guay, P. & Tremolières, S. (2011). Contactless Low Resolution Angular Sensor. *Proc. Of the 14th ESMATS, 2011.* ESA SP-698, European Space Agency, Noordwijk, The Netherlands.